



ELSEVIER

Physics Reports 337 (2000) 157–169

PHYSICS REPORTS

www.elsevier.com/locate/physrep

Electroconvection in homeotropically aligned nematics

Á. Buka^{a,*}, P. Tóth^{a,b}, N. Éber^a, L. Kramer^b

^aResearch Institute for Solid State Physics and Optics, H-1525 Budapest, P.O. Box 49, Hungary

^bPhysikalisches Institut, Universität Bayreuth, D-95444 Bayreuth, Germany

Abstract

Recent experimental results on electroconvection in homeotropic nematic liquid crystals are summarized. Static and dynamic properties of the patterns at and above threshold are discussed. The azimuthal angle of the director is determined for various pattern morphologies (normal, abnormal and CRAZY rolls). Preliminary results on controlled defect motion are presented. © 2000 Elsevier Science B.V. All rights reserved.

PACS: 05.45. – a

Keywords: Electroconvection; Liquid crystals; Pattern formation

1. Introduction

Electroconvection (EC) in planar nematics [1,2] belongs among the first observed pattern forming processes in liquid crystals [3]. As a result of extensive studies in the past decades, the main characteristics of the phenomenon are well understood [4–7].

In homeotropically aligned nematics with negative dielectric anisotropy (ϵ_a) the first instability that occurs when applying an AC electric field parallel to the director is the bend Freedericksz transition [8]. The deformed director configuration involves a homogeneous tilt and an arbitrary azimuthal angle. This continuous degeneracy can conveniently be lifted by applying a magnetic field perpendicular to the electric one. Electroconvection (EC) sets in on the distorted state and no preferred roll direction is expected (in the absence of magnetic field) because of the rotational symmetry of the boundary conditions.

Efforts to investigate homeotropically oriented cells using nematics with manifestly negative ϵ_a were initiated rather recently, see [9–18] for experimental and [6,20–24] for theoretical work.

In this work results on normal (NR), oblique (OR) and abnormal (AR) rolls are summarized.

* Corresponding author.

E-mail address: ab@szfki.hu (Á. Buka).

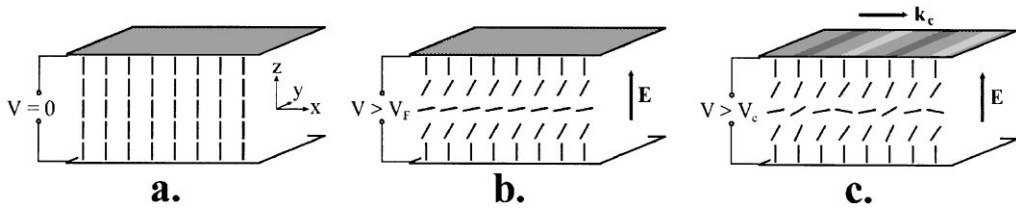


Fig. 1. Geometry and director distribution in a homeotropic cell: (a) $0 \leq V < V_F$ – homeotropic texture; (b) $V_F < V < V_c$ – Freedericksz distorted state; and (c) $V_c < V$ electroconvection pattern.

The threshold of convection, the wave number at onset, and the threshold for the transition between order and disorder in the presence of a stabilizing magnetic field have been measured and compared with theory. Whereas in the oblique roll range the behaviour of the correlation time of the disordered state exhibits the expected scaling behaviour near onset, the disordered state in the normal roll range at zero magnetic field shows no dynamics below a well defined value of the control parameter, in contrast to the theoretical predictions. At that value one has reproducibly a continuous and reversible transition to a dynamic state which goes hand in hand with the appearance of chevron-like structures.

An experimental technique is presented for visualizing the domain structure of AR-s. The voltage and frequency dependence of the azimuthal angle of the director is determined. A new striped pattern (CRAZY rolls) is observed and characterized in a parameter range.

Defect dynamics of the roll pattern is studied as a function of the magnetic field.

2. Freedericksz distorted state

In the homeotropic geometry the director is initially parallel to z and this state is isotropic (rotationally symmetric) in the x – y plane (Fig. 1a). The first instability at a voltage $V = V_F$ is the (ideally) spatially homogeneous (in the x – y plane) bend Freedericksz transition where the director bends away from the z direction, singling out spontaneously a local direction in the x – y plane (Fig. 1b). This corresponds to a spontaneous breaking of the $O(2)$ symmetry, and leads to a Goldstone mode, i.e. an undamped mode describing the (infinitesimal) rotation of the in-plane director. Large-scale variations are weakly damped. As a consequence, one observes point defects (umbilics).

The isotropy can be broken externally by applying a weak stabilizing magnetic field (a field strength much smaller than the bend Freedericksz threshold H_F suffices) parallel to the plane of the sample (in the x direction) which defines the direction of the bend. There remains a twofold degeneracy of the Freedericksz distorted state with walls separating the two types of domains.

3. Threshold behaviour

At higher voltages $V_c > V_F$ there is a transition to electroconvection (Fig. 1c, where V_c is frequency-dependent contrary to V_F , see Fig. 2a), which is in many respects similar to that in cells with planarly aligned nematics. However, the presence of the Goldstone mode in the homeotropic case with full rotational invariance (i.e. without additional magnetic field) leads to fundamental

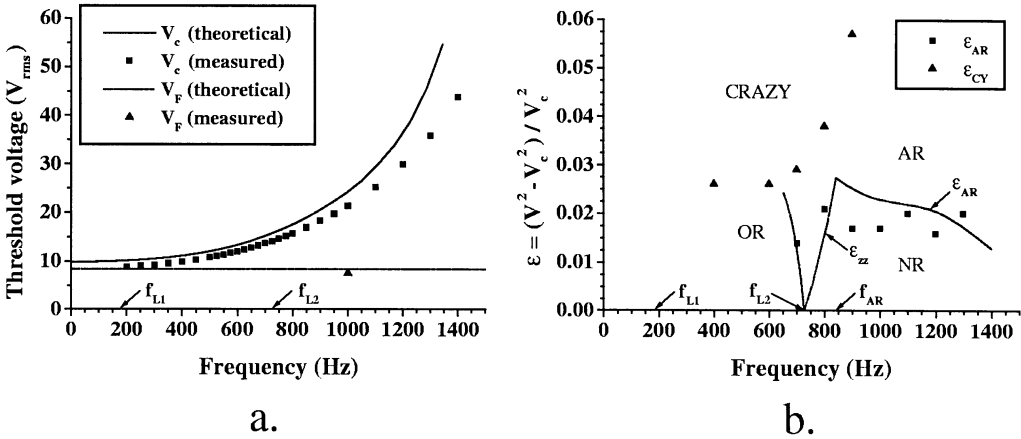


Fig. 2. a. Frequency dependence of the Fredericksz and the EC threshold voltages. b. Phase diagram for EC scenarios. Measured points refer to a 31 μm thick homeotropic cell of Nematic Phase 5A (Merck) at $H = H_F/3$, lines correspond to theoretical calculations.

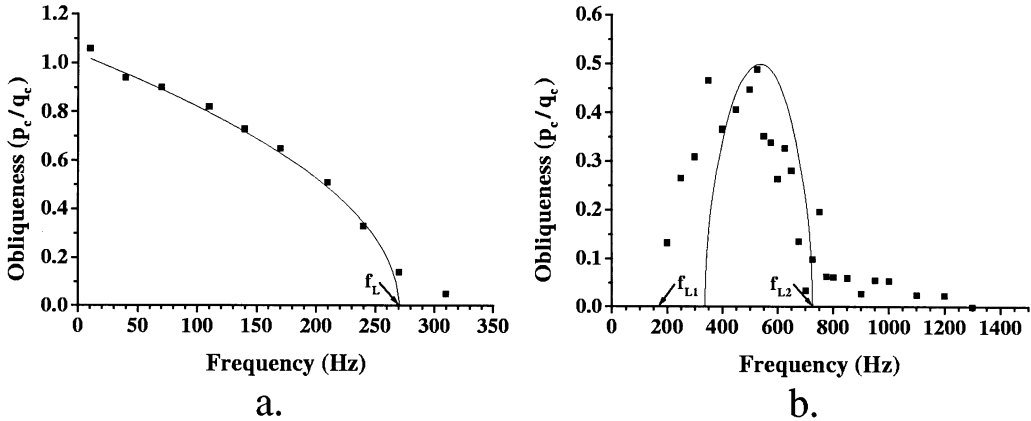


Fig. 3. Frequency dependence of the obliqueness of the rolls (p_c/q_c). Solid lines correspond to theoretical calculations, measured points refer to: (a) a 47 μm thick homeotropic cell of MBBA at $H = 0$; and (b) a 31 μm thick homeotropic cell of Nematic Phase 5A (Merck) at $H = H_F/3$.

differences. In fact the patterns are disordered. Nevertheless normal (NR), oblique (OR) and abnormal (AR) rolls can be distinguished.

Since the convective flow is coupled to periodic distortions of the director, the pattern is easily visualized [25]. The patterns at threshold are characterized by a two-dimensional (local) wave vector $\mathbf{k}_c = (q_c, p_c)$, describing the orientation and spacing of the rolls (q_c and p_c are the x and y components of \mathbf{k}_c , x is the local direction of the in-plane director). \mathbf{k}_c can be determined from a 2D Fourier analysis of the snapshots of the pattern inspite of the fact that the rolls have arbitrary orientation. The ratio p_c/q_c characterizes the obliqueness of the rolls and vanishes at the Lifshitz point f_L (Fig. 3).

The threshold behaviour is well described by a linear stability analysis (LSA) of the basic (nonconvecting but Fredericksz distorted) state starting from the standard hydrodynamic

equations [20]. This analysis cannot capture nonlinear properties like e.g. the amplitude of the pattern as a function of the reduced control parameter commonly defined as $\varepsilon = V^2/V_c^2 - 1$.

If the degeneracy of the azimuthal angle of the director is lifted by applying a magnetic field electroconvection scenarios similar to those in planar arrangement can be observed. The magnetic field $\mathbf{H}||x$ acts on the patterns by stabilizing the in-plane director orientation (for not too large ε , see below) [14–16,21,22]. The patterns have the appearance of regularly ordered normal (typically above a frequency f_L) or oblique (below f_L) rolls.

Besides producing well ordered patterns H shifts V_c upwards and changes also the critical wave vector. In particular, f_L is shifted to lower frequencies and k_c is increased. Similarly to the planar configuration, the roll angle shows near f_L a square root behaviour with frequency (Fig. 3a) [26]. However, certain combinations of the material parameters may lead (e.g. in Nematic Phase 5A, Merck) to the appearance of a second (lower) Lifshitz point, i.e. to normal rolls at very low frequencies (Fig. 3b). Such a behaviour has never been observed in planarly aligned samples.

4. Static and dynamic convection states slightly above threshold

The next step is a weakly nonlinear analysis, which employs an expansion in terms of the complex amplitude A of the patterning mode including slow modulations in space and time. In the NR regime this leads to a Ginzburg–Landau-type amplitude equation [5,6]. In addition, in the presence of a weak orienting magnetic field the in-plane director mode described by an angle φ must be included [21,23]. The theory predicts destabilization of NRs either by a zig-zag (undulatory) instability slightly above f_L (or f_{L2}) or by a transition to ARs (see below) above a frequency f_{AR} . In Fig. 2b this scenario is shown for the material Merck Phase 5A at $H = H_F/3$. There is a general scaling $\varepsilon \sim H^2$ in the range of validity of the weakly nonlinear theory. For larger H a more general theory starting from the basic hydrodynamic equations has to be used [27].

The zig-zag destabilization at ε_{zz} has been observed in MBBA, where the interval between f_{AR} and f_L is larger than in Phase 5 [26]. Slightly above ε_{zz} one has stable undulations, at larger values ε_u (depending on the magnetic field) defects appear. The disordered state attained beyond ε_u appears to be static in the NR range (in contrast to the theoretical prediction). In other experiments on the material MBBA a slow dynamics was found [15,16].

The frozen state and its transition to dynamics has been studied in detail at zero magnetic field (where $\varepsilon_u = 0$) [26]. For $\varepsilon > \varepsilon_u$ defects (dislocations in the roll pattern) appear which order along chains (Fig. 4). The topological charge of defects alternates from chain to chain. There is a remarkable similarity between this structure and the chevrons known in the dielectric range of planar samples. A theoretical connection between the two structures has been made [21,24]. The density of defects in the homeotropic chevron state has been measured as a function of ε and a fairly sharp increase at $\varepsilon_s > \varepsilon_u$ was detected. At ε_s also a dynamical state took place [26].

The time evolution of the patterns and the transition from static to dynamic disorder was studied without magnetic field as a function of ε and f . To characterize the director dynamics quantitatively the autocorrelation function of the measured intensity was constructed and the correlation time was determined by assuming exponential decay (Fig. 5) [26]. At ε_s one seems to have a sharp and reversible crossover between the stationary and dynamic states, thus indicating a forward bifurcation. The temporal behaviour was found significantly different in the OR range

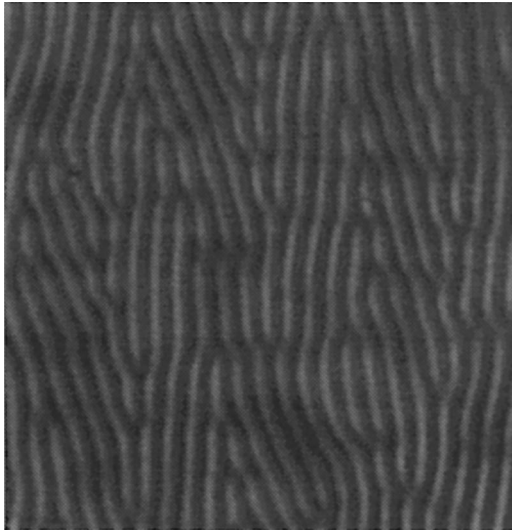


Fig. 4. Chevrons in the conductive regime of a homeotropic sample.

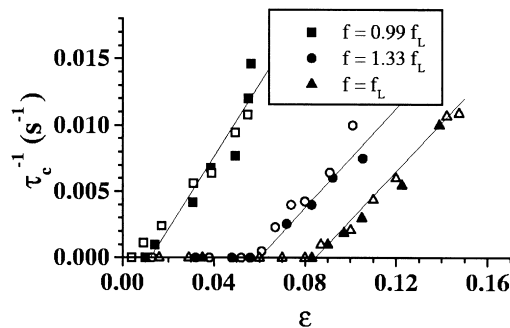


Fig. 5. Epsilon dependence of the correlation time constant for various frequencies around f_L . Solid symbols refer to a 23 μm thick homeotropic cell of MBBA at $H = 0$ measured with increasing, open symbols with decreasing voltage, lines correspond to a linear fit. $\epsilon_s = 0.012, 0.085$ and 0.060 for $f = 0.99f_L, f_L$ and $1.33f_L$, respectively.

below f_L , where ϵ_s was found to be zero (or nearly zero). In agreement with the theory which predicts spatio-temporal chaos at onset, we find that the inverse correlation time is proportional with ϵ .

5. Abnormal and CRAZY rolls

For $f > f_{AR}$ the destabilization of normal rolls occurs at ϵ_{AR} through a homogeneous pitchfork bifurcation leading to ARs where the in-plane director is rotated homogeneously in the x - y plane out of its normal orientation ($\varphi \neq 0$) [21,23] (Fig. 2b). Finally, at higher ϵ defects appear which move irregularly through the patterns (defect turbulence). The in-plane director angle can

be given as

$$\varphi_{\pm} = \begin{cases} \pm \Phi \sqrt{\varepsilon - \varepsilon_{AR}} & (\varepsilon > \varepsilon_{AR}), \\ 0 & (\varepsilon < \varepsilon_{AR}), \end{cases} \quad (1)$$

where $\Phi = (\zeta_{yy} q_c)^{-1}$ diverges at $f \rightarrow f_L$.

Abnormal rolls have been found first in homeotropic liquid crystals where increasing the applied voltage in the normal roll regime the director may suffer an azimuthal rotation away from the roll normal without affecting the direction of the rolls [11,13,17,19]. This new scenario has been observed in planar geometry too [7]. Theoretical descriptions of the phenomenon could also be given both for the homeotropic [21,23] and the planar case [7].

Due to the strong anchoring in planar cells the distortion of the director from the roll normal in ARs results in a twist deformation. The adiabatic propagation of light makes it difficult to detect this twist (depolarization techniques should be used) [28,29]. In contrast to this, as there is no constraint on the azimuthal angle of the director at a homeotropic surface, a similar deviation should yield a net rotation of the optical axis of the homeotropic sample. The local azimuthal angle of the director can thus easily be mapped optically by simply adjusting the polarization of the illuminating light. Thus, the homeotropic geometry has considerable advantages over the planar one in detecting ARs.

The snapshots and the x - α images in Fig. 6 illustrate the experimentally observed NR-AR scenarios. In the subcritical ($\varepsilon < 0$) and the normal roll ($0 < \varepsilon < \varepsilon_{AR}$) regimes the director is homogeneously oriented along the magnetic field ($\varphi(x) = 0$).

In the abnormal roll regime ($\varepsilon_{AR} < \varepsilon < \varepsilon_{CY}$) φ becomes nonzero and slowly spatially modulated (without influencing the roll direction). φ varies continuously on a length scale of several roll wavelengths (no sharp domain walls) [30].

Just above ε_{AR} (when φ is small) the AR domains are fairly large and patchy (Fig. 7a). At higher ε the domains get thinner and elongated mainly along the roll direction and they become more and more periodic (Figs. 6b and 7b). This feature is clearly demonstrated by the histograms in Figs. 7c and d exhibiting the distribution of domain widths of the snapshots. The typical domain width is 3-6 times the roll wavelength, and is decreasing with increasing ε .

The size and location of the AR domains fluctuates on the time scale of seconds. However, the total area of the two types of domains is equal in average, i.e. there is no preference for either the plus or the minus sign of φ .

The voltage dependence of the maximum (φ_+) and minimum (φ_-) of $\varphi(x)$ (Figs. 8a and b) exhibits the pitchfork bifurcation expected from Eq. (1). The opening angle of the pitchfork is increasing sharply as the frequency approaches f_L from above, which is also in accordance with the theory [30].

When the in-plane director angle becomes large enough (about $\pm 20 - 30^\circ$), which occurs only for frequencies not too far from f_L , a new striped structure – the CRAZY rolls (convection in a regular array of z - y disclination loops)¹ – evolves and grows along the rolls replacing partially the ARs (Fig. 6c). The width of a single CRAZY unit is about the wavelength of the ARs.

¹ Name and structure for CRAZY rolls were proposed in Ref. [30].

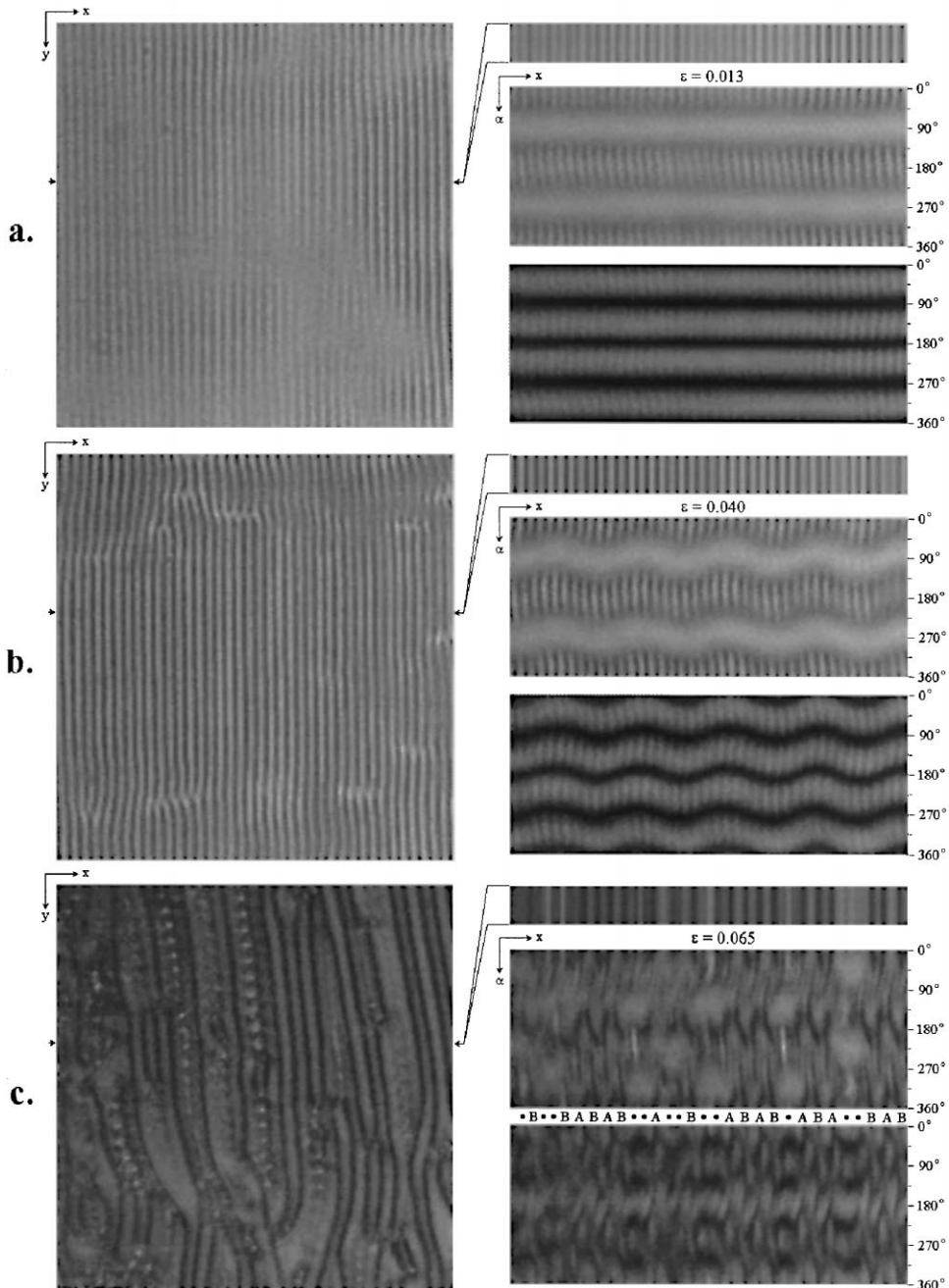


Fig. 6. NRs (a), ARs (b) and CRAZY rolls (c) for Phase 5A, cell thickness $d = 31 \mu\text{m}$, $H = H_F/3$, $f > f_L$. Left column: snapshots with polars parallel to x . Right column: $x-\alpha$ images (actually $x-t$ images for polars rotating with a fixed angular velocity) taken with parallel (middle right), and at crossed polars (bottom right). The top right image exhibits the pattern along the tested line with polars parallel to x . (a) normal rolls ($f = 1000 \text{ Hz}$); (b) ‘periodically’ alternating AR domains ($f = 1000 \text{ Hz}$); and (c) CRAZY rolls ($f = 800 \text{ Hz}$). A and B represent the two symmetry degenerate versions of CRAZY units, (●) stands for an abnormal roll.

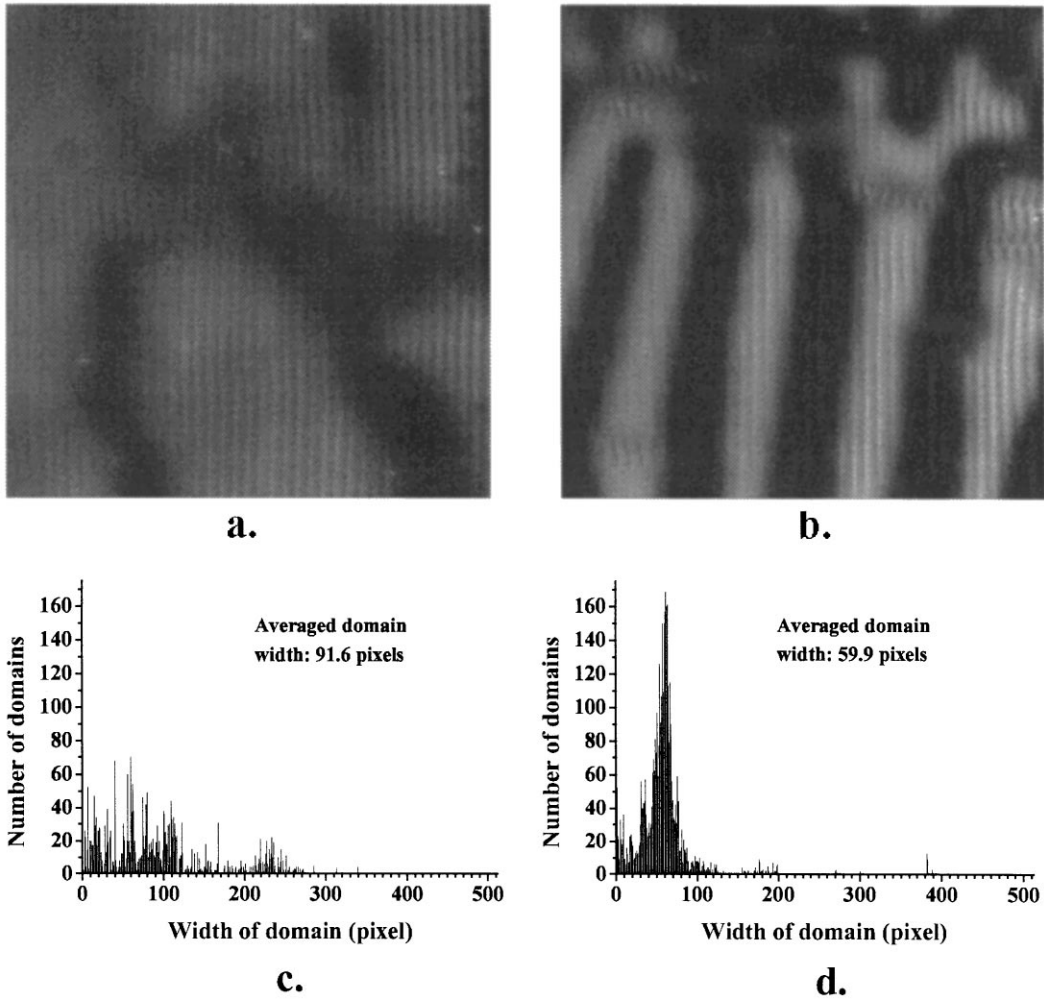


Fig. 7. Snapshots of abnormal roll patterns at $f > f_L$ and distribution of horizontal domain widths (crossed polars, polarizer rotated to 8° away from x). Same conditions as in Fig. 6b except $f = 1200$ Hz. (a,c) small $\varepsilon - \varepsilon_{AR}$, patchy domains; (b,d) larger $\varepsilon - \varepsilon_{AR}$, ‘periodic’ domains.

In each unit of CRAZY rolls the in-plane angle changes by $\pm 90^\circ$ when passing through its width, in contrast to the AR domains where the in-plane director angle varies smoothly over length scales of multiples of the roll wavelength. There are two types of CRAZY units as the direction of rotation can be either from $+45^\circ$ to -45° (type A), or vice versa (type B). The CRAZY rolls can either fill the space densely by themselves, then the units of type A and B alternate regularly, or are separated by domains without disclinations (Fig. 6c). The separating domains either appear like the usual rolls (ARs) or have a modulation in y -direction. In the separating domains bordered by CRAZY units of identical type the azimuthal angle changes smoothly by $\pm 90^\circ$, otherwise the net rotation of the in-plane director is zero.

Increasing ε above ε_{AR} CRAZY units are born locally one by one, and then grow along the rolls into the ARs. Reducing ε below ε_{AR} the decay of CRAZY rolls often leaves behind long disclination

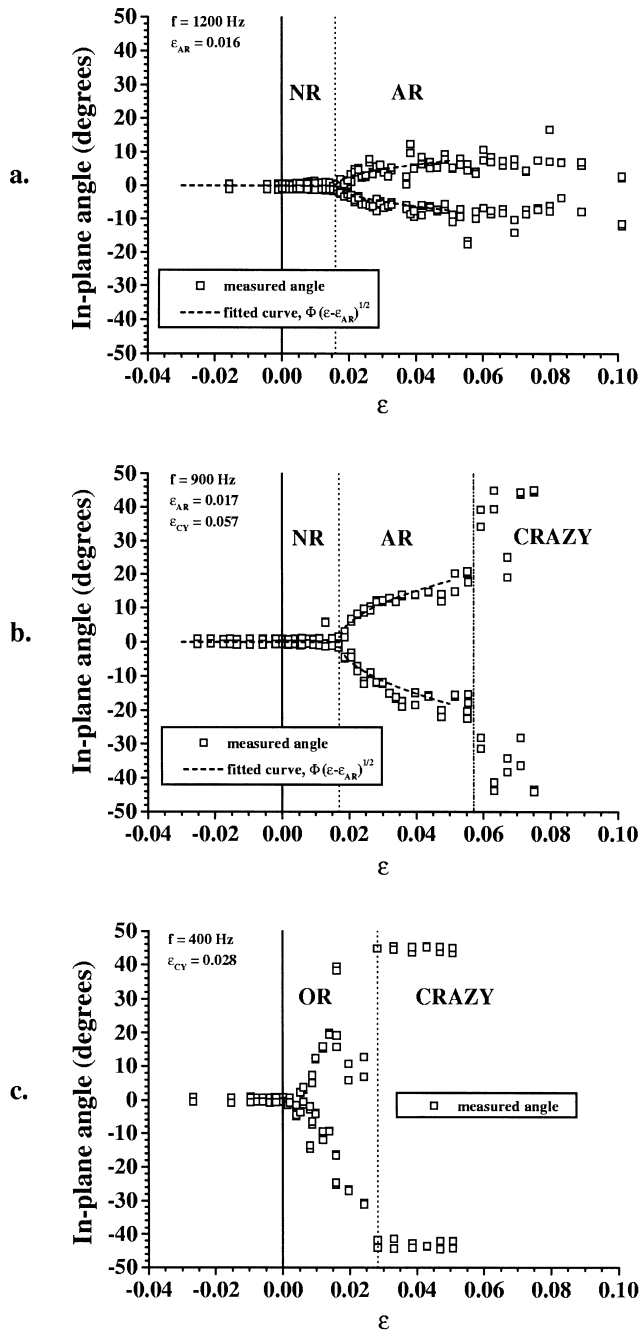


Fig. 8. ε -dependence of the maximum and minimum of $\varphi(x)$ in a $31 \mu\text{m}$ thick homeotropic cell of Nematic Phase 5A (Merck) at $H = H_F/3$. The dashed line represents a fit to the theoretical predictions (Eq. (1)). The vertical lines separate the various scenarios: (a) $f \gg f_L$; (b) $f > f_L$; and (c) $f < f_L$.

loops, which can temporarily persist even in the subcritical voltages. They relax on the time scale of several minutes.

These observations have led us to the conclusion that each CRAZY unit contains two disclination lines running along the roll direction at (or near) the surfaces and these lines are finally closing at the tips forming a loop [30]. The coexistence between CRAZY rolls and ARs shows that convection still plays an important role.

It should be mentioned that a period doubling of the roll pattern leading to striped domains that appear similar to a periodic packing of A and B CRAZY units has recently been reported in another substance [31].

At frequencies below f_L oblique rolls are observed. As the sign of the roll angle is arbitrary, there should be zig and zag domains separated by sharp domain walls. According to the theory in oblique rolls, instead of a pitchfork bifurcation, one always has a nonzero in-plane director angle, which behaves like ε^2 for small ε and should increase monotonically with ε . The sign of φ is opposite in the zig and the zag domains. The measured ε -dependence of φ shown in Fig. 8c is consistent with this prediction. The jump in φ at $\varepsilon = \varepsilon_{CY}$ indicates a transition in the structure. Though the optical appearance of the resulting new structure differs slightly from that of the CRAZY rolls, they are characterized by the same type of rotation of the in-plane director angle, as for $f > f_L$.

6. Dynamics of defects

The motion of defects (dislocations) in ordered roll patterns in anisotropic systems constitutes a mechanism for the change of the wavevector \mathbf{k} of the pattern. In fact ‘climb’ (motion along the rolls) will change the spacing, i.e. the wavenumber perpendicular to the rolls. ‘Glide’ (motion perpendicular to the rolls) will change the orientation, i.e. the wavenumber parallel to the rolls. Near the primary threshold, where the system behaves like a potential system, one has an optimal wavevector \mathbf{k}_{id} . Motion of defects will be such that the wavevector mismatch $\Delta\mathbf{k} = \mathbf{k} - \mathbf{k}_{id}$ decreases. The precise connection between $\Delta\mathbf{k}$ and the velocity v of a defect has been calculated within the Ginzburg–Landau description valid near threshold [32,33]. The relation $\Delta v(k)$ is nonlinear and involves a logarithmic singularity for $\Delta k \rightarrow 0$. The direction of v should always be perpendicular to $\Delta\mathbf{k}$.

In this context experiments have been performed in EC of planarly aligned LCs [34–36]. Quantitative experiments involved only changes of the roll spacing where one has pure climb. The defect velocity was found to be consistent with the theory but detailed feature, like the logarithmic singularity could not be resolved.

The homeotropic system studied here provides an elegant method to investigate glide: the preferred direction is defined by the applied magnetic field in the plane of the sample. One can vary this direction by rotating the field with respect to the cell. So there is a possibility of varying $\mathbf{k}/|\mathbf{k}|$, i.e. to induce glide.

A defect pair was created in the NR regime by heating the cell locally with a He–Ne laser. Then the cell was rotated by an angle α with respect to the magnetic field which created a mismatch $\Delta\mathbf{k} = 2\mathbf{k} \sin \alpha/2$ (Fig. 9). As expected, defect motion with a main *glide*-component was observed. The velocity of the defects was measured during a time period, when the distance between the two

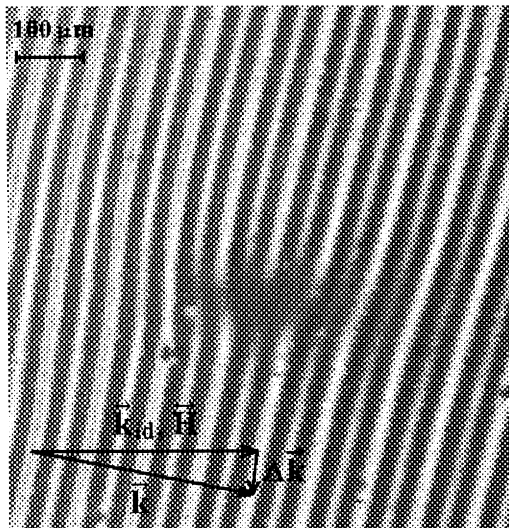


Fig. 9. Snapshot of a defect (dislocation) in the electroconvection pattern.

defects was large enough, that interaction could be neglected. The velocity v was determined by taking a series of digitized images and localizing the defect position by a demodulation method [36]. This was done before reorientation of the pattern due to other processes became appreciable.

In order to compare the results of these measurements quantitatively with theory the coefficients of the Ginzburg–Landau amplitude equation had to be determined: necessary information has been extracted from the slope of the defect core and the decay time of the patterns as was done in [36]. Preliminary results confirm the predicted direction of defect movement and indicate the presence of the logarithmic term in the relation between velocity and the wavevector mismatch. Detailed results will be presented elsewhere.

7. Outlook

Clearly, there remains much room for further study. There is the marked discrepancy between experiment and theory concerning the frozen, disordered patterns in the NR range where theory predicts a dynamical state. In order to test if pinning due to inhomogeneities of the alignment of the bounding plates is involved, one could repeat the experiments with thicker cells where pinning is expected to play a smaller role.

In Section 5, the scenario leading from NRs to ARs and CRAZY rolls was monitored by increasing ϵ at fixed H . It would seem useful to keep ϵ fixed at some small value and decrease H , because in this way one remains within the range of validity of the weakly nonlinear theory. We point out that a similar procedure can be envisaged in planar systems. Thereby, applying a magnetic field perpendicular to the director alignment one should be able to reduce ϵ_{AR} until it reaches zero at the twist Freedericksz threshold field.

Acknowledgements

We wish to thank W. Pesch and A.G. Rossberg for discussions. Support of the Hungarian Research Grants Nos. OTKA-T031808, OTKA-T022772, VW Foundation and the EU TMR Research Network “Patterns, Noise and Chaos” is gratefully acknowledged. A.B. and L.K. thank the hospitality of the “Max-Planck-Institut für Physik Komplexer Systeme”, Dresden.

References

- [1] V. Freedericksz, V. Tsvetkov, *Acta Physicochim. URSS* 3 (1935) 879.
- [2] R. Williams, *J. Chem. Phys.* 39 (1963) 384.
- [3] Á. Buka, L. Kramer (Eds.), *Pattern Formation in Liquid Crystals*, Springer, Berlin, 1995.
- [4] W. Helfrich, *J. Chem. Phys.* 51 (1969) 4092.
- [5] E. Bodenschatz, W. Zimmermann, L. Kramer, *J. Phys. France* 49 (1988) 1875.
- [6] L. Kramer, W. Pesch, in: Á. Buka, L. Kramer (Eds.), *Pattern Formation in Liquid Crystals*, Springer, Berlin, 1995.
- [7] E. Plaut, W. Decker, A.G. Rossberg, L. Kramer, W. Pesch, A. Belaidi, R. Ribotta, *Phys. Rev. Lett.* 79 (1997) 2367; E. Plaut, W. Pesch, *Phys. Rev. E* 59 (1999) 1277.
- [8] S. Chandrasekhar, *Liquid Crystals*, Cambridge University Press, Cambridge, 1992; P.G. de Gennes, J. Prost, *The Physics of Liquid Crystals*, Clarendon Press, Oxford, 1993; L.M. Blinov, *Electrooptical and Magneto-optical Properties of Liquid Crystals*, Wiley, New York, 1983.
- [9] D. Meyerhofer, A. Sussman, *Appl. Phys. Lett.* 20 (1972) 337.
- [10] M.I. Barnik, L.M. Blinov, M.F. Grebenkin, S.A. Pikin, V.G. Chigrinov, *J. Exp. Theor. Phys. URSS* 69 (1975) 1080.
- [11] H. Richter, Á. Buka, I. Rehberg, *Mol. Cryst. Liq. Cryst.* 251 (1994) 181.
- [12] H. Richter, Á. Buka, I. Rehberg, *Phys. Rev. E* 51 (1995) 5886.
- [13] H. Richter, Á. Buka, I. Rehberg, in: *Spatio-Temporal Patterns in Nonequilibrium Complex Systems*, P. Cladis, P. Palfy-Muhoray (Eds.), Addison-Wesley, Reading, MA, 1994.
- [14] H. Richter, N. Klöpper, A. Hertrich, Á. Buka, *Europhys. Lett.* 30 (1995) 37.
- [15] Sh. Kai, K. Hayashi, Y. Hidaka, *J. Phys. Chem.* 100 (1996) 19007; Y. Hidaka, J. Huh, K. Hayashi, M. Tribelsky, Sh. Kai, *J. Phys. Soc. Japan* 66 (1997) 3329.
- [16] Y. Hidaka, J.-H. Huh, K. Hayashi, Sh. Kai, Tribelsky M, *Phys. Rev. E* 56 (1997) R6256.
- [17] J.-H. Huh, Y. Hidaka, Sh. Kai, *Phys. Rev. E* 58 (1998) 7355.
- [18] J.-H. Huh, Y. Hidaka, Sh. Kai, *J. Phys. Soc. Japan* 67 (1998) 1948.
- [19] J.-H. Huh, Y. Hidaka, Sh. Kai, *J. Phys. Soc. Japan* 68 (1999) 1567.
- [20] A. Hertrich, W. Decker, W. Pesch, L. Kramer, *J. Phys. France II* 2 (1992) 1915; L. Kramer, A. Hertrich, W. Pesch, in: Sh. Kai (Ed.), *Pattern Formation in Complex Dissipative Systems*, World Scientific, Singapore, 1992.
- [21] A.G. Rossberg, A. Hertrich, L. Kramer, W. Pesch, *Phys. Rev. Lett.* 76 (1996) 4729; A.G. Rossberg, L. Kramer, *Physica Scripta* T67 (1996) 121.
- [22] A. Hertrich, Ph.D. Thesis, Bayreuth, 1995.
- [23] A.G. Rossberg, Ph.D. Thesis, Bayreuth, 1997.
- [24] A.G. Rossberg, L. Kramer, *Physica D* 115 (1998) 19.
- [25] S. Rasenat, G. Hartung, B.L. Winkler, I. Rehberg, *Exp. Fluids* 7 (1989) 412.
- [26] P. Tóth, Á. Buka, J. Peinke, L. Kramer, *Phys. Rev. E* 58 (1998) 1983.
- [27] A. Hertrich, W. Pesch, unpublished.
- [28] H. Amm, M. Grigutsch, R. Stannarius, *Mol. Cryst. Liq. Cryst.* 320 (1998) 11.
- [29] S. Rudroff, H. Zhao, L. Kramer, I. Rehberg, *Phys. Rev. Lett.* 81 (1998) 4144.
- [30] A.G. Rossberg, N. Éber, Á. Buka, *Phys. Rev. E* 61 (2000) R25.
- [31] C. Fradin, P.L. Finn, H.R. Brand, P.E. Cladis, *Phys. Rev. Lett.* 81 (1998) 2902.

- [32] E. Bodenschatz, W. Pesch, L. Kramer, *Physica D* 32 (1988) 135; L. Kramer, E. Bodenschatz, W. Pesch, Comment in *Phys. Rev. Lett.* 64 (1990) 2588.
- [33] L. Pismen, *Vortices in Nonlinear Fields: from Liquid Crystals to Superfluids, from Non-equilibrium Patterns to Cosmic Strings*, Clarendon Press, Oxford, 1999.
- [34] S. Nasuno, S. Takeuchi, Y. Sawada, *Phys. Rev. A* 40 (1989) 3457.
- [35] Sh. Kai, N. Chizumi, M. Kohno, *Phys. Rev. A* 40 (1989) 6554.
- [36] S. Rasenat, V. Steinberg, I. Rehberg, *Phys. Rev. A* 42 (1990) 5998.